

# FIBER QUADRISECANTS IN KNOT ISOTOPIES

T. FIEDLER AND V. KURLIN

ABSTRACT. Fix a straight line  $L$  in Euclidean 3-space and consider the fibration of the complement of  $L$  by half-planes. A generic knot  $K$  in the complement of  $L$  has neither fiber quadriseccants nor fiber extreme secants such that  $K$  touches the corresponding half-plane at 2 points. Both types of secants occur in generic isotopies of knots. We give lower bounds for the number of these fiber secants in all isotopies connecting given isotopic knots. The bounds are expressed in terms of invariants calculable in linear time with respect to the number of crossings.

## 1. INTRODUCTION

In this paper we give another application of the main result of [3], namely the *higher order* Reidemeister theorem for one-parameter families of knots. Fix a straight line  $L$  in  $\mathbb{R}^3$ , the *axis*. For simplicity assume that  $L$  is horizontal. Consider the fibration  $\varphi : \mathbb{R}^3 - L \rightarrow S^1_\varphi$  by half-planes attached to the axis  $L$ . The fibration  $\varphi$  can be visualized as an open book whose half-planes are fibers of  $\varphi$ . We will study some distances between isotopic knots in the complement  $\mathbb{R}^3 - L$ .

A knot is the image of a  $C^\infty$ -smooth embedding  $S^1 \rightarrow \mathbb{R}^3 - L$ . An isotopy of knots is a smooth family  $\{K_t\}$ ,  $t \in [0, 1]$ , of smooth knots. The theory of knots in  $\mathbb{R}^3 - L$  covers the classical knot theory in  $\mathbb{R}^3$  and closed braids. An  $n$ -braid  $\beta$  is a family of  $n$  disjoint strands in a vertical cylinder such that the strands have fixed endpoints on the horizontal bases of the cylinder and they are monotonic in the vertical direction. After identifying the bases of the cylinder in Fig. 1, any braid  $\beta$  converts into the *closed* braid  $\hat{\beta}$ , a link in a solid torus going around the axis  $L$ . The boundary circle of the lower base of the cylinder plays the role of  $L \cup \infty$ .

A *secant*, a *triseccant* and a *quadriseccant* of  $K \subset \mathbb{R}^3 - L$  is a straight line meeting  $K$  transversally in 2, 3 and 4 points, respectively. A secant meeting  $K$  in points  $p, q$  is *extreme* if the secant and the tangents of  $K$  at  $p, q$  lie in a common plane. Namely,  $K$  has tangencies of *order* 1 at  $p, q$  with a plane passing through the secant, i.e. the plane and  $K$  are given by  $\{z = 0\}$  and  $\{y = 0, z = x^2\}$  in some local coordinates near  $p, q$ . A generic knot has finitely many extreme secants and quadriseccants. If we are interested only in fiber secants respecting  $\varphi$  then these geometric features define codimension 1 singularities in the space of all smooth knots  $K \subset \mathbb{R}^3 - L$ .

**Definition 1.1.** A *fiber* secant, a *fiber* triseccant, a *fiber* quadriseccant of a knot  $K \subset \mathbb{R}^3 - L$  is a straight line meeting  $K$  transversally in 2, 3, 4 points, respectively, that lie in a fiber of the fibration  $\varphi : \mathbb{R}^3 - L \rightarrow S^1_\varphi$ . A fiber secant meeting  $K$  in points  $p, q$  is called *extreme* if  $K$  has tangencies of order 1 at  $p, q$  with the fiber.

---

*Date:* January 30, 2007.

*2000 Mathematics Subject Classification.* 57M25.

*Key words and phrases.* Knot, braid, isotopy, fiber quadriseccant, fiber extreme secant, writhe, trace graph, tetrahedral move, higher order Reidemeister theorem.

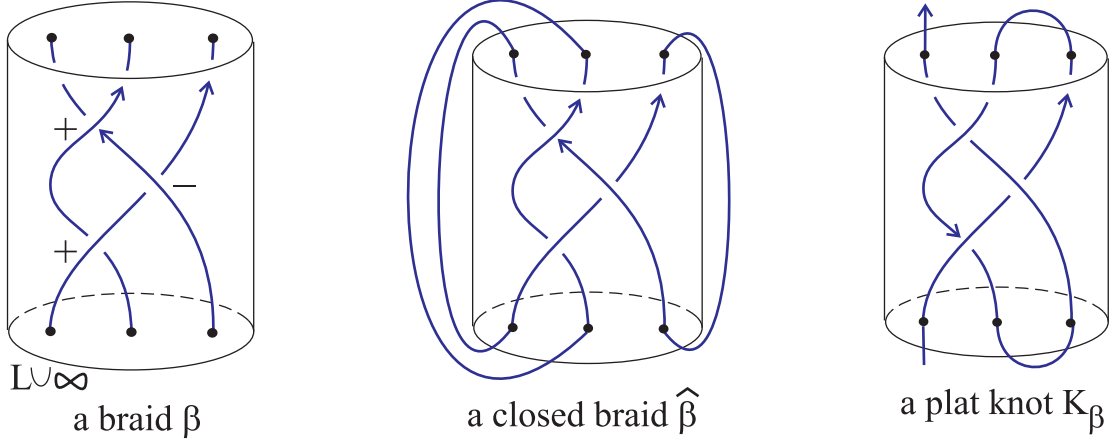


FIGURE 1. Examples of a braid, a closed braid, a plat knot.

We use fiber secants to measure a distance between different embeddings of a knot. A similar distance with respect to Reidemeister moves of type III was studied in [1], see Fig. 4. Reidemeister moves can be performed on a knot  $K$  in a small neighbourhood of a disk. Reidemeister moves III correspond to triple points in the horizontal disk of a projection, i.e. to vertical trisecants meeting  $K$  in 3 points.

So the authors of [1] found the minimal number of vertical trisecants in isotopies between different representations of a knot. We consider more general features of a knot, namely quadriseccants in the half-planes of the fibration  $\varphi$  and estimate their minimal number in knot isotopies. Arbitrary quadriseccants provide lower bounds for the ropelength of knots [2]. To define our lower bounds we associate to each knot  $K \subset \mathbb{R}^3 - L$  an oriented graph  $\text{TG}(K)$ , the *trace graph* in a thickened torus.

Choose cylindrical coordinates  $\rho, \varphi, \lambda$  in  $\mathbb{R}^3$ , where  $\lambda$  is the coordinate in the oriented axis  $L$ ,  $\rho$  and  $\varphi$  are polar coordinates in a plane orthogonal to  $L$ . For an ordered pair of points  $(p, q) \subset \{\varphi = \text{const}\}$ , let  $\tau(p, q)$  be the angle between  $L$  and the oriented line  $S(p, q)$  passing first through  $p$  and after through  $q$ . Denote by  $\rho(p, q)$  the distance between  $S(p, q)$  and the origin  $0 \in L$ . Introduce the oriented thickened torus  $\mathbb{T} = S_\tau^1 \times S_\varphi^1 \times \mathbb{R}_\rho^+$  parametrized by  $\tau, \varphi \in [0, 2\pi)$  and  $\rho \in \mathbb{R}^+$ .

**Definition 1.2.** Take a knot  $K \subset \mathbb{R}^3 - L$  in general position such that  $K$  intersects each fiber of  $\varphi$  in finitely many points. Map an ordered pair  $(p, q) \subset K \cap \{\varphi = \text{const}\}$  to  $(\tau(p, q), \varphi, \rho(p, q)) \in \mathbb{T}$ . So each oriented fiber secant of  $K$  maps to a point in the thickened torus  $\mathbb{T}$ . The image of this map is the *trace graph*  $\text{TG}(K) \subset \mathbb{T}$ .

Figure 2 shows the trace graph  $\text{TG}(K)$  of a long trefoil  $K$  going once around a very long circle  $L \cup \infty$ . The fibers there are horizontal planes. The knots in Fig. 2 are obtained from  $K$  by the rotation around a vertical line. A crossing in the projection of a rotated knot corresponds to a fiber secant of  $K$ , i.e. to a point of  $\text{TG}(K)$ . The embedding  $\text{TG}(K) \subset \mathbb{T}$  is symmetric under the shift  $\tau \mapsto \tau + \pi$ .

For a generic knot  $K$  of Definition 2.1,  $\text{TG}(K)$  can have only *hanging* vertices and *triple* vertices associated to fiber tangents and fiber trisecants of  $K$ , respectively. A double crossing of  $\text{TG}(K)$  under  $\text{pr}_{\tau\varphi} : \text{TG}(K) \rightarrow S_\tau^1 \times S_\varphi^1$  corresponds to a pair of parallel secants meeting  $K$  in points that lie in a fiber  $\{\varphi = \text{const}\}$ .

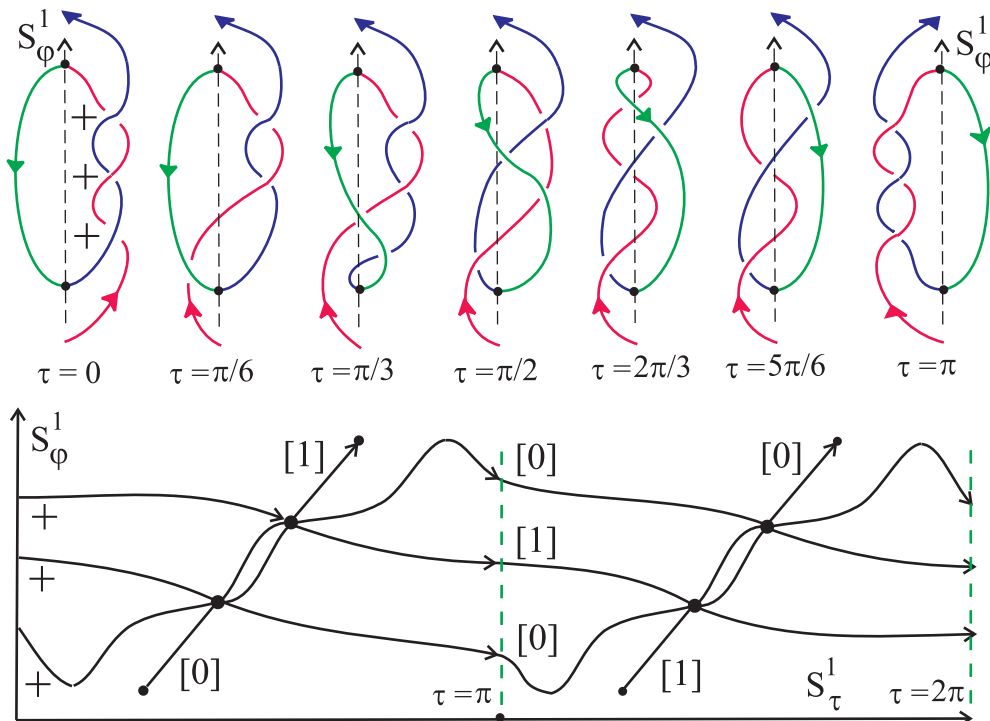


FIGURE 2. The trace graph  $TG(K)$  of the long trefoil  $K$ .

Let  $m$  be the linking number of a knot  $K$  with the axis  $L$ . It turns out that the trace graph  $TG(K)$  splits into a union of oriented *traces* (arcs or circles) marked by canonically defined homological markings in  $\mathbb{Z}_{|m|}$ , where  $\mathbb{Z}_0 = \mathbb{Z}$  and  $\mathbb{Z}_1 = \{0\}$ , see Definition 2.2. For example, the closure of  $\sigma_3\sigma_2\sigma_1 \in B_4$  has the trace graph in Fig. 3, which is a disjoint union of 3 trace circles marked by  $[1], [2], [3] \in \mathbb{Z}_4$ .

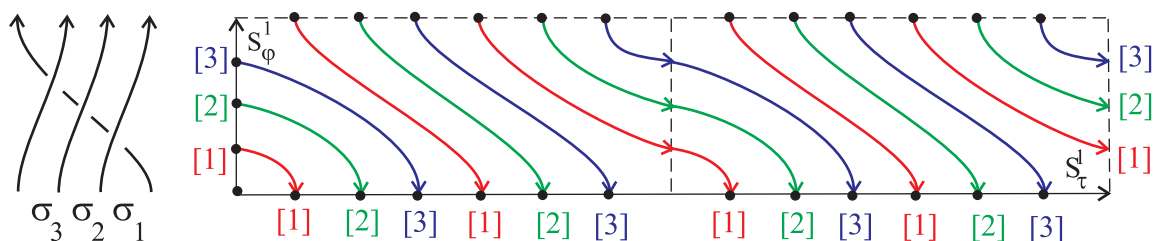


FIGURE 3. The trace graph of  $\widehat{\sigma_3\sigma_2\sigma_1}$  splits into 3 trace circles.

Introduce the *sign* of a crossing in the projection  $\text{pr}_{\tau\varphi}(TG(K))$  as usual, see Fig. 1. We shall define 3 functions on  $TG(K)$ , which will be invariant under regular isotopy of  $TG(K)$ , not allowing Reidemeister moves of type I, see Lemma 3.1.

**Definition 1.3.** Take a knot  $K \subset \mathbb{R}^3 - L$  such that  $\text{lk}(K, L) = m \neq \pm 1$  and the projection  $\text{pr}_{\tau\varphi}(TG(K))$  has finitely many crossings. For distinct  $[a], [b] \in \mathbb{Z}_{|m|} - \{0\}$ , the *unordered* writhe  $W_{a,b}^u(K)$  is the sum of signs over all crossings of the trace marked by  $[a]$  with the trace marked by  $[b]$ . The *ordered* writhe  $W_{a,b}^o(K)$  is the sum of signs over all crossings, where the trace  $[a]$  overcrosses the trace  $[b]$ . The *coordinated* writhe  $W_{a,a}^c(K)$  is the sum of signs over all self-crossings of the trace  $[a]$ .

We do not consider knots  $K \subset \mathbb{R}^3 - L$  with  $\text{lk}(K, L) = \pm 1$ , because in this case  $\text{TG}(K)$  splits into trace arcs marked by [0] and [1] only, see Definition 2.2. The trace graph  $\text{TG}(K)$  is constructed from a plane projection of  $K$ , see Lemma 2.4. The writhes of Definition 1.3 depend on a geometric embedding  $K \subset \mathbb{R}^3 - L$ , but can be computed in linear time with respect to the number of crossings of  $K$  and change under knot isotopies in a controllable way, see Lemma 3.2.

**Theorem 1.4.** *For isotopic generic knots  $K_0, K_1 \subset \mathbb{R}^3 - L$ , denote by  $\text{fqs}(K_0, K_1)$  and  $\text{fes}(K_0, K_1)$  the minimum number of fiber quadriseccants and fiber extreme secants, respectively, occurring during all isotopies  $\{K_t\}$ ,  $t \in [0, 1]$ .*

*For isotopic knots  $K_0, K_1$ , we have  $\text{fqs}(K_0, K_1) \geq \frac{1}{12} \sum_{0 \neq a \neq b \neq 0} |W_{a,b}^u(K_0) - W_{a,b}^u(K_1)|$*

*and  $\text{fqs}(K_0, K_1) + \frac{1}{6} \text{fes}(K_0, K_1) \geq \frac{1}{12} \sum_{a \neq 0} |W_{a,a}^c(K_0) - W_{a,a}^c(K_1)|$ . Given isotopic*

*closed braids  $\hat{\beta}_0, \hat{\beta}_1$ , we get  $\text{fqs}(\hat{\beta}_0, \hat{\beta}_1) \geq \frac{1}{12} \sum_{0 \neq a \neq b \neq 0} |W_{a,b}^o(\hat{\beta}_0) - W_{a,b}^o(\hat{\beta}_1)|$ .*

The third lower bound is not less than the first one, but works for closed braids only. The second bound gives another estimate for the number of fiber quadriseccants for closed braids since fiber extreme secants do not occur in braid isotopies.

## 2. THE TRACE GRAPH OF A KNOT

We shall define generic knots  $K \subset \mathbb{R}^3 - L$  and geometric features of knots, considered as codimension 1 singularities in the space of all knots in  $\mathbb{R}^3 - L$ . Each singularity is illustrated by a small portion of the projection of  $K$  along the corresponding secant. For example, a tangent of  $K$  maps to a cusp in the plane projection of  $K$  along the tangent, while a quadriseccant projects to a quadruple point.

**Definition 2.1.** A knot  $K \subset \mathbb{R}^3 - L$  is *generic* if  $K$  has no following features:

$\ast$  : a fiber quadriseccant intersecting  $K$  transversally in 4 points;

$\times$  : a fiber triseccant meeting  $K$  in 3 points such that the secant lies in the plane spanned by the tangents of  $K$  at 2 of these points;

$\succ$  : a fiber secant meeting  $K$  in 2 points and having a tangency of order 1 with  $K$  at one of these points;

$\mathcal{J}$  : a fiber secant meeting  $K$  in points  $p, q$  such that  $K$  has a tangency of *order 2* at  $p$  with the plane spanned by the secant and the tangent of  $K$  at  $q$ , i.e. the plane and  $K$  are given by  $\{z = 0\}$  and  $\{y = 0, z = x^3\}$  in local coordinates near  $p$ ;

$\curvearrowright$  : a fiber tangent having a tangency of *order 2* with  $K$ , i.e. the tangent and  $K$  are given by  $\{y = z = 0\}$  and  $\{y = 0, x^2 = z^5\}$  in local coordinates;

$\times, \mathcal{K}$  : a fiber triseccant meeting  $K$  in 3 points such that  $K$  has a tangency of order 1 with the fiber at one of these points;

$\prec$  : a fiber tangent meeting  $K$  in a point, where  $K$  has a tangency of *order 2* with the fiber, i.e. the fiber and  $K$  are given locally by  $\{z = 0\}$  and  $\{y = 0, z = x^3\}$ ;

$\succ, \mathcal{M}$  : a fiber secant meeting  $K$  in 2 points, where  $K$  has tangencies of order 1 with the fiber.

The singularities of Definition 2.1 can be visualized by rotating a knot around a vertical axis. The last singularity represents two local extrema with same vertical coordinate: they collide under the projection after rotating by a suitable angle.

A *trace* in the trace graph  $TG(K)$  of a knot  $K$  is either a subarc ending at hanging vertices or a subcircle of  $TG(K)$ . A trace passes through triple vertices without changing its direction. The trace graph in Fig. 2 consists of 2 trace arcs.

By Definition 1.2 any point in  $TG(K)$  corresponds to a fiber secant of  $K$  and also to an intersection in the projection of  $K$  along the secant. Recall that hanging vertices and triple vertices of  $TG(K)$  correspond to cusps and triple intersections. Mark also *tangent* vertices of degree 2 in  $TG(K)$  such that the corresponding secant projects to a tangent point of order 1, see 2 tangent vertices in Fig. 6iv.

All points of  $TG(K)$  apart from the vertices of  $TG(K)$  correspond to double crossings with well-defined signs. Associate to such a point the *sign* of the corresponding crossing in the projection. While we travel along a trace of  $TG(K)$  the sign does not change at triple vertices, but switches at tangent vertices.

Let us look at the function  $\tau$  on fiber secants passing through 2 points  $p, q \in K$ . Namely,  $\tau(p, q)$  is the angle between  $L$  and the fiber secant through  $p, q$ . The function  $\tau(p, q)$  has a local extremum if and only if the corresponding secant of  $K$  projects to a tangent point, i.e.  $\tau$  changes its monotonic type at tangent vertices of  $TG(K)$ .

**Definition 2.2.** Take a generic knot  $K \subset \mathbb{R}^3 - L$  with  $lk(K, L) = m$ . Split  $TG(K)$  by tangent vertices into arcs with associated signs coming from plane projections. Orient each arc so that if the angle  $\tau$  is increasing (respectively, decreasing) along the arc then the associated sign of the arc is  $+1$  (respectively,  $-1$ ), see Fig. 2.

Any point of  $TG(K)$  apart from the vertices of  $TG(K)$  is associated to a crossing  $(p, q)$  in the projection of  $K$  along the secant through  $p, q \in K$ . Smoothing the projection at  $(p, q)$  produces a 2-component link. The linking number of  $L$  with the component, where the undercrossing goes to the overcrossing, is called the *homological marking*  $[a] \in \mathbb{Z}_{|m|}$  of  $(p, q)$  and of the point of  $TG(K)$ , see Fig. 3.

The trace graph in Fig. 2 splits into 2 trace arcs marked by  $[0]$  and  $[1]$ . Under the shift  $\tau \mapsto \tau + \pi$ , the homological marking  $[a]$  converts into  $[|m| - a] \in \mathbb{Z}_{|m|}$ , see Fig. 3. Recall that a hanging vertex of  $TG(K)$  corresponds to a fiber tangent of  $K$ , i.e. to an ordinary cusp in the plane projection along this tangent.

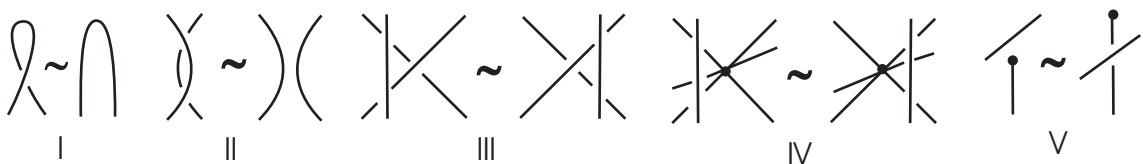


FIGURE 4. Reidemeister moves for trace graphs.

**Lemma 2.3.** *The trace graph  $TG(K)$  of a generic knot  $K$  splits into traces with well-defined homological markings. The orientation of edges, introduced in Definition 2.2, provides orientations of all traces of  $TG(K)$ .*

*Proof.* Consider the sign of a crossing, monotonic type of the function  $\tau$  and homological marking as functions of a point in the trace graph  $TG(K)$ . All these functions

remain constant while the projection of  $K$  along the corresponding secant keeps its combinatorial type. By the classical Reidemeister theorem, a knot projection can change under Reidemeister moves of types I, II, III, see Fig. 4.

Under Reidemeister move I a fiber secant of  $K$  appears or disappears, i.e. the corresponding point in the trace graph comes to a hanging vertex of  $\text{TG}(K)$ . Under Reidemeister move II, two crossings with opposite signs and same marking appear or disappear. At this moment the function  $\tau$  reverses its monotonic type. So the orientations of adjacent arcs of  $\text{TG}(K)$  agree at tangent vertices. Under Reidemeister move III nothing changes, i.e. all arcs of a trace have same marking.  $\square$

The right picture in Fig. 1 shows a *plat* diagram of a knot  $K_\beta$  associated to a braid  $\beta$ . Any knot can be isotoped to a curve with a plat diagram.

**Lemma 2.4.** *Let  $K_\beta$  be a knot with a plat diagram associated to a  $(2n + 1)$ -braid  $\beta$  of length  $l$ . The trace graph  $\text{TG}(K_\beta)$  can be constructed combinatorially from the diagram of  $K_\beta$ . The writhes of Definition 1.3 can be computed with complexity  $Cln^2$ .*

*Proof.* Describe the trace graphs of elementary braids containing one crossing only. Figure 5 shows the explicit example for the crossing  $\sigma_1$  of first two strands in the 4-braid. Firstly we draw all strands in a vertical cylinder. Secondly we approximate with the first derivative the strands forming a crossing by smooth arcs.

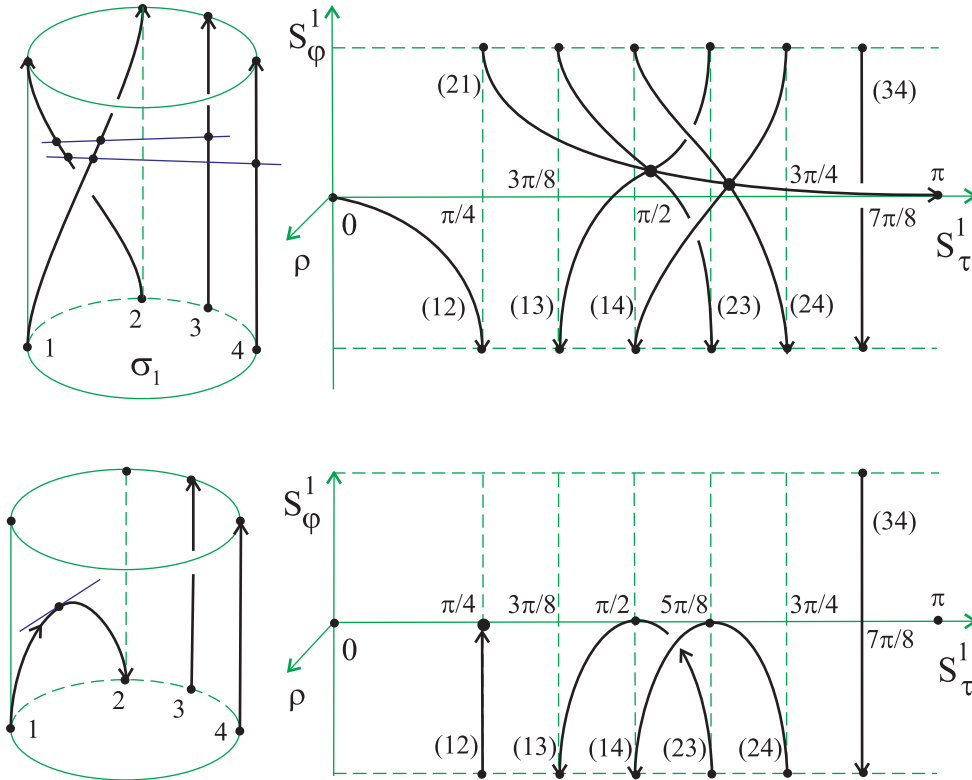


FIGURE 5. Half trace graphs of  $\sigma_1 \in B_4$  and a local maximum.

The monotonic strands on the left pictures in Fig. 5 are denoted by 1,2,3,4. The trace graphs on the right pictures have arcs labelled by ordered pairs  $(ij)$ ,  $i, j \in \{1, 2, 3, 4\}$ . The arc  $(ij)$  represents crossings, where the  $i$ th strand overcrosses the  $j$ th one. For instance, at the moment  $\tau = 0$  the braid  $\sigma_1$  has exactly one crossing

(12), which becomes a crossing (21) after rotating the braid by  $\tau = \pi/4$ . Two triple vertices on the upper right picture correspond to two horizontal trisecants on the upper left picture in Fig. 5. Similarly we construct the trace graph of a local extremum. The only hanging vertex corresponds to a horizontal tangent.

In general we split  $K_\beta$  by fibers of  $\varphi : \mathbb{R}^3 - L \rightarrow S_\varphi^1$  into several sectors each of that contains exactly one crossing or one extremum. To each sector we associate the corresponding elementary block and glue them together. The resulting trace graph contains  $2l(2n - 1)$  triple vertices and  $2n$  hanging vertices. Any two arcs in an elementary block have at most one crossing, i.e. not more than  $n^2$  crossings in total. Hence each writhe of Definition 1.3 can be computed with complexity  $Cln^2$ .  $\square$

**Definition 2.5.** Denote by  $\Omega$  the discriminant of knots  $K$  failing to be generic due to one of the singularities of Definition 2.1. An isotopy of knots  $\{K_t\}$ ,  $t \in [0, 1]$ , is *generic* if the path  $\{K_t\}$  intersects  $\Omega$  transversally. A *regular* isotopy of trace graphs is generated by the Reidemeister moves of types II, III, IV, V in Fig. 4.

Any orientations and symmetric images of the moves in Fig. 4 are allowed. Proposition 2.6 is a particular case of a more general higher order Reidemeister theorem [3, Theorem 1.8]. A knot can be reconstructed from its trace graphs equipped with labels, ordered pairs of integers, see details in [3, section 5].

**Proposition 2.6.** *If knots  $K_0, K_1 \subset \mathbb{R}^3 - L$  are isotopic then  $TG(K_0), TG(K_1)$  are related by regular isotopy and a finite sequence of the moves in Fig. 6.*

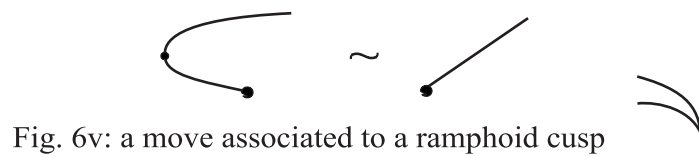
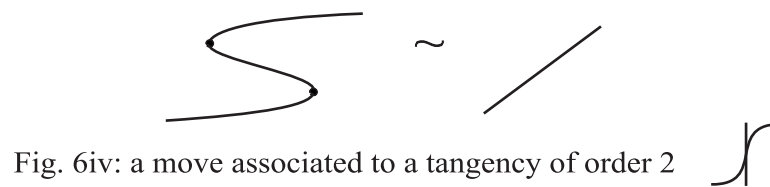
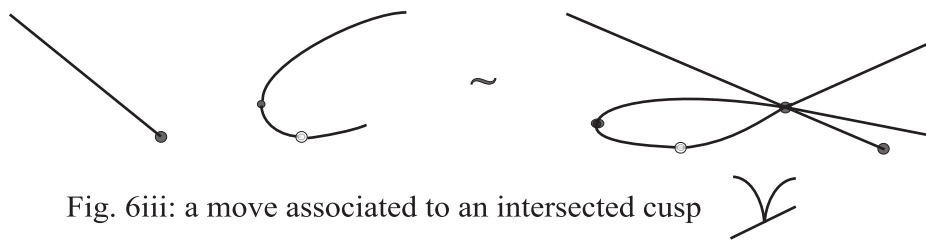
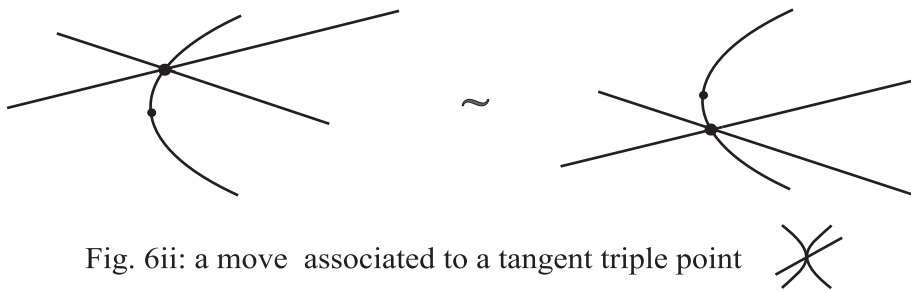
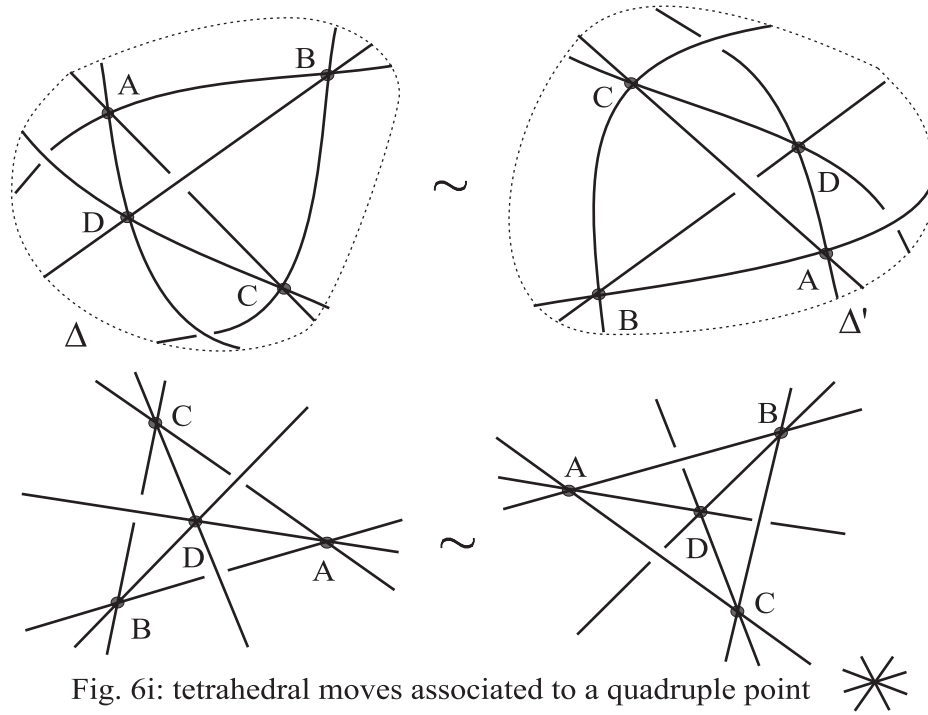
*Proof.* The singularities of Definition 2.4 are all codimension 1 singularities associated to fiber secants and fiber tangents of knots, see [3, section 3]. Any isotopy of knots can be approximated by a generic isotopy of Definition 2.5. Each move of Fig. 6 corresponds to one of the singularities. For instance, when a path in the space of knots passes through a knot with a fiber quadrisequant, the tetrahedral move 6i changes the trace graph by collapsing and blowing up a tetrahedron. A formal correspondence between the singularities and moves was shown in [3, Claim 4.5]. Empty vertices of degree 2 in Fig. 6 denote points corresponding to the singularity  $\clubsuit$ , where a knot touches a fiber and has a fiber secant through this tangent point.

The moves of Fig. 6 keep the orientation and homological markings of traces. If three traces marked by  $[a], [b], [c]$  meet in a triple vertex then  $b = a + c \pmod{|m|}$ , where  $[b]$  is the marking of the middle trace, see a more general case in [3, Lemma 6.3]. The trace graph always remains symmetric under  $\tau \mapsto \tau + \pi$ . Hence each move of Fig. 6 describes how to replace a small disk  $\Delta$  and the symmetric image of  $\Delta$  under  $\tau \mapsto \tau + \pi$  by another small disk  $\Delta'$  and the symmetric image of  $\Delta'$ , respectively.  $\square$

### 3. PROOFS OF MAIN RESULTS

**Lemma 3.1.** *The writhes of Definition 1.3 are invariant under regular isotopy of trace graphs in the sense of Definition 2.5.*

*Proof.* The Reidemeister moves of types II, III and IV in Fig. 4 do not change the sum of signs in the writhes. The Reidemeister move of type V either adds or deletes a crossing of  $TG(K)$ , but a trace arc coming to a hanging vertex always has homology marking  $[0]$  modulo  $|\text{lk}(K, L)|$  and is excluded in Definition 1.3.  $\square$





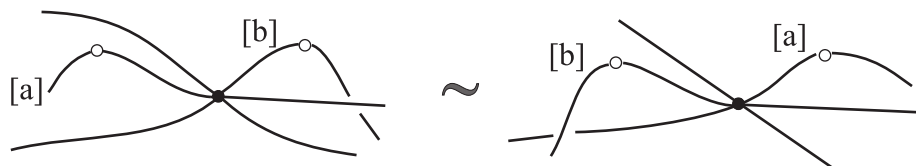


Fig. 6vi: a move associated to a horizontal triple intersection

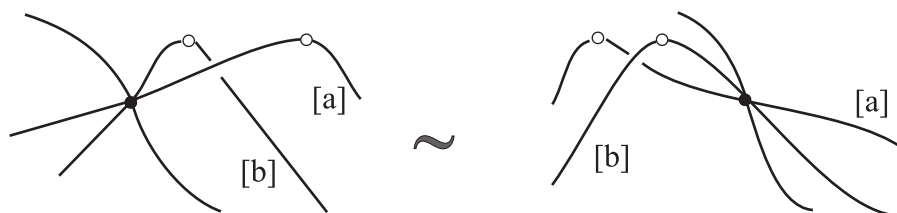


Fig. 6vii: a move associated to a horizontal triple intersection

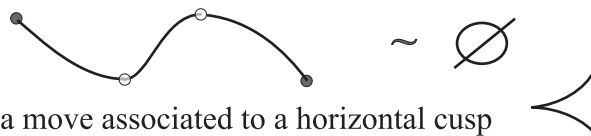


Fig. 6viii: a move associated to a horizontal cusp

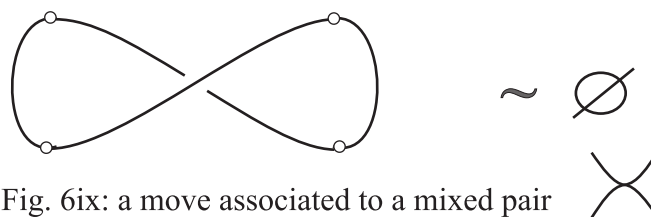


Fig. 6ix: a move associated to a mixed pair

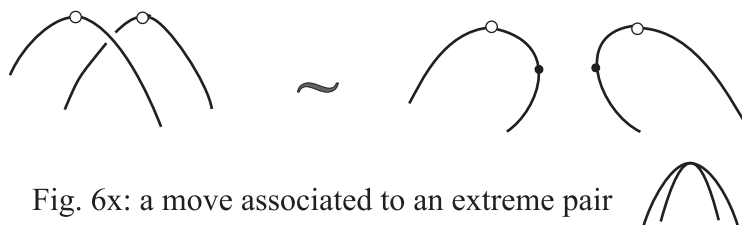


Fig. 6x: a move associated to an extreme pair

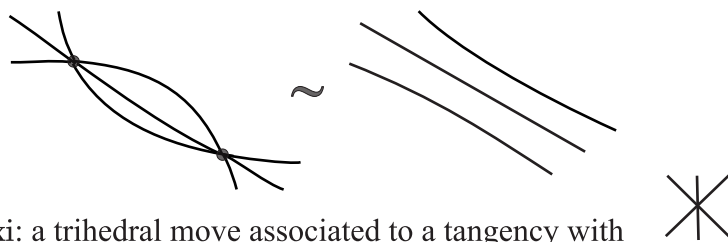


Fig. 6xi: a trihedral move associated to a tangency with

FIGURE 6. Moves on trace graphs


**Lemma 3.2.** *The moves in Fig. 6 keep the writhes of Definition 1.3 except*

- *the move 6i changes  $W_{a,b}^u$  ( $a \neq b$ ) by  $\pm 2$  for at most 6 unordered pairs  $\{a, b\}$ ;*
- *the move 6i changes  $W_{a,b}^o$  ( $a \neq b$ ) by  $\pm 1$  for at most 12 ordered pairs  $(a, b)$ ;*
- *the move 6i changes  $W_{a,a}^c$  either (1) by  $\pm 6$  for at most 2 values of  $a$ , or (2) by  $\pm 4$  for at most 2 values of  $a$  and by  $\pm 2$  for at most 2 values of  $a$ , or (3) by  $\pm 2$  for at most 6 values of  $a$ ;*
- *the moves 6vi, 6vii change  $W_{a,b}^o$  ( $a \neq b$ ) by  $\pm 1$  for at most 4 ordered pairs  $(a, b)$ ;*
- *the moves 6ix and 6x change  $W_{a,a}^c$  by  $\pm 1$  for at most two values of  $a$ .*

*Proof.* The move 6i switches exactly 3 couples of symmetric crossings. For instance, the arc  $DB$  overcrosses  $AC$  in the left picture of Fig. 6i, but  $DB$  undercrosses  $AC$  in the right picture. Hence, for at most 6 unordered pairs  $\{a, b\}$  with  $a \neq b$ , the unordered writhe  $W_{a,b}^u$  changes by  $\pm 2$ . Similarly, for at most 12 ordered pairs  $(a, b)$ , the ordered writhe  $W_{a,b}^o$  changes by  $\pm 1$  since exactly one crossing of a trace  $[a]$  over a trace  $[b]$  either appears or disappears under the move 6i.

If all 3 crossings in the disk  $\Delta$  in Fig. 6i are formed by traces with same homological marking  $[a]$  then the coordinated writhes  $W_{a,a}^c$  and  $W_{|m|-a, |m|-a}^c$  change by  $\pm 6$  as required in the case (1). If two of the above crossings are formed by a trace  $[a]$  and the remaining one by a different trace  $[b]$  then we arrive at the case (2). The case (3) arises when each of the 3 crossings in  $\Delta$  is formed by a different trace.

In the moves 6vi and 6vii the overcrossing arc becomes undercrossing and vice versa, but the sign of the crossing is invariant, i.e.  $W_{a,b}^u$  does not change. Each of the moves 6vi and 6vii deletes exactly one crossing, where a trace  $[a]$  overcrosses a trace  $[b]$ , and adds another crossing, where the trace  $[a]$  undercrosses the trace  $[b]$ . Under the symmetry  $\tau \mapsto \tau + \pi$ , we get similar conclusions for the traces marked by  $[|m| - a]$  and  $[|m| - b]$ . So the ordered writhe  $W_{a,b}^o$  changes by  $\pm 1$  for the 4 ordered pairs  $(a, b)$ ,  $(b, a)$  and  $(|m| - a, |m| - b)$ ,  $(|m| - b, |m| - a)$ .

The move 6ix adds or deletes a crossing of a trace circle  $[a]$  with itself. Hence only the writhes  $W_{a,a}^c$  and  $W_{|m|-a, |m|-a}^c$  change by  $\pm 1$ . The move 6x adds or deletes a crossing between two arcs belonging to traces with same homological marking  $[a]$ . Indeed, a pair of crossings corresponding to these arcs looks like in a horizontal version  of Reidemeister move II, see Fig. 4. By Definition 2.2 the markings of these crossings are equal. So the conclusion is the same as for the move 6ix.  $\square$

**Proof of Theorem 1.4.** To prove the first lower bound it suffices to show that the right hand side increases by 1 only if a generic isotopy  $\{K_t\}$  passes through a knot with a fiber quadrisequant. By Lemma 3.2 the unordered writhe changes under the move 6i associated to a fiber quadrisequant, see the correspondence between singularities and moves in [3, section 4]. Six unordered pairs  $\{a, b\}$  provide the maximal increase 1 as required. Lemma 3.2 also proves the third lower bound since only the moves 6i, 6ii, 6iv, 6xi are relevant for braids.

For the second lower bound, we are interested in crossings, where arcs have same marking. By Lemma 3.2 the coordinated writhe changes only under the move 6i and two moves 6ix, 6x associated to a fiber extreme secant in knot isotopies. Under the move 6i the right hand side increases at most by 1 while under the moves 6ix and 6x the maximal increase is  $1/6$  after multiplying by  $1/12$ .  $\square$

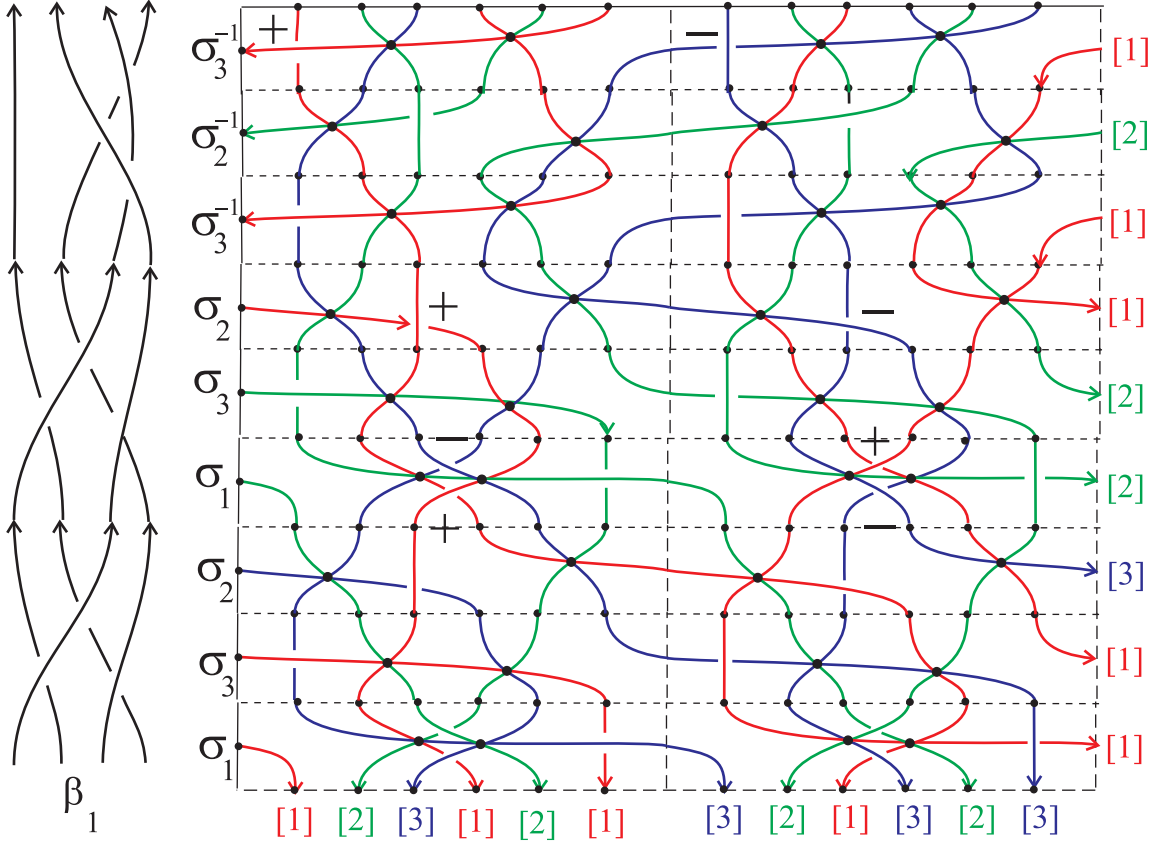


FIGURE 7. The trace graph of the closure of  $\beta_1 = (\sigma_1\sigma_3\sigma_2)^2\sigma_3^{-1}\sigma_2^{-1}\sigma_3^{-1}$ .

**Example 3.3.** Consider the isotopic closures of the braids  $\beta_0 = \sigma_3\sigma_2\sigma_1$  and  $\beta_1 = (\sigma_1\sigma_3\sigma_2)^2\sigma_3^{-1}\sigma_2^{-1}\sigma_3^{-1}$ . The trace graphs of  $\hat{\beta}_0$  and  $\hat{\beta}_1$  are in Fig. 3,7, respectively. They were constructed by attaching elementary blocks described in the proof of Lemma 2.4. So we assume that the closed braids are given by embeddings into a neighbourhood of the torus  $S^1_\tau \times S^1_\varphi$  located vertically in  $\mathbb{R}^3 - L$ .

Both graphs split into 3 closed traces (circles with self-intersections) marked by [1],[2],[3]. The trace graph in Fig. 3 has no crossings, i.e. the writhes of Definition 1.3 vanish. For the trace graph of  $\hat{\beta}_1$ , the non-zero writhes are  $W_{1,1}^c = 4$ ,  $W_{3,3}^c = -4$ . The 4 signs + and 4 signs - are shown in Fig. 7. The second lower bound of Theorem 1.4 implies that any isotopy connecting the closed braids  $\hat{\beta}_0, \hat{\beta}_1$  involves at least one fiber quadrisequant. The conclusion is the same for the closures of  $\beta_0\gamma, \beta_1\gamma$ , where  $\gamma$  is any pure 4-braid.

Consider the 4-braid  $\beta = (\sigma_1\sigma_3\sigma_2)^2(\sigma_1^{-1}\sigma_3^{-1}\sigma_2^{-1})^2$  in Fig. 8 and the sequence of the braids  $\beta_n = \beta^{n-1}\beta_1$ ,  $n \geq 1$ , whose closures are isotopic to  $\hat{\beta}_0$ , see Fig. 3. Fig. 8 contains the part of  $TG(\hat{\beta}_n)$  corresponding to a single factor  $\beta$  in  $\beta_n$ . So  $TG(\hat{\beta}_n)$  is obtained from  $TG(\hat{\beta}_1)$  by inserting  $n - 1$  copies of Fig. 8 at the bottom of Fig. 7. The part in Fig. 8 has the writhes  $W_{1,1}^c = 3$  and  $W_{3,3}^c = -3$ . Hence  $TG(\hat{\beta}_n)$  has  $W_{1,1}^c = 3n + 1$  and  $W_{3,3}^c = -3n - 1$ . By Theorem 1.4 any isotopy connecting the closures of  $\beta_0$  and  $\beta_n$  involves at least  $\frac{3n + 1}{12}$  fiber quadrisequants. So the second lower bound of Theorem 1.4 can be arbitrarily large.

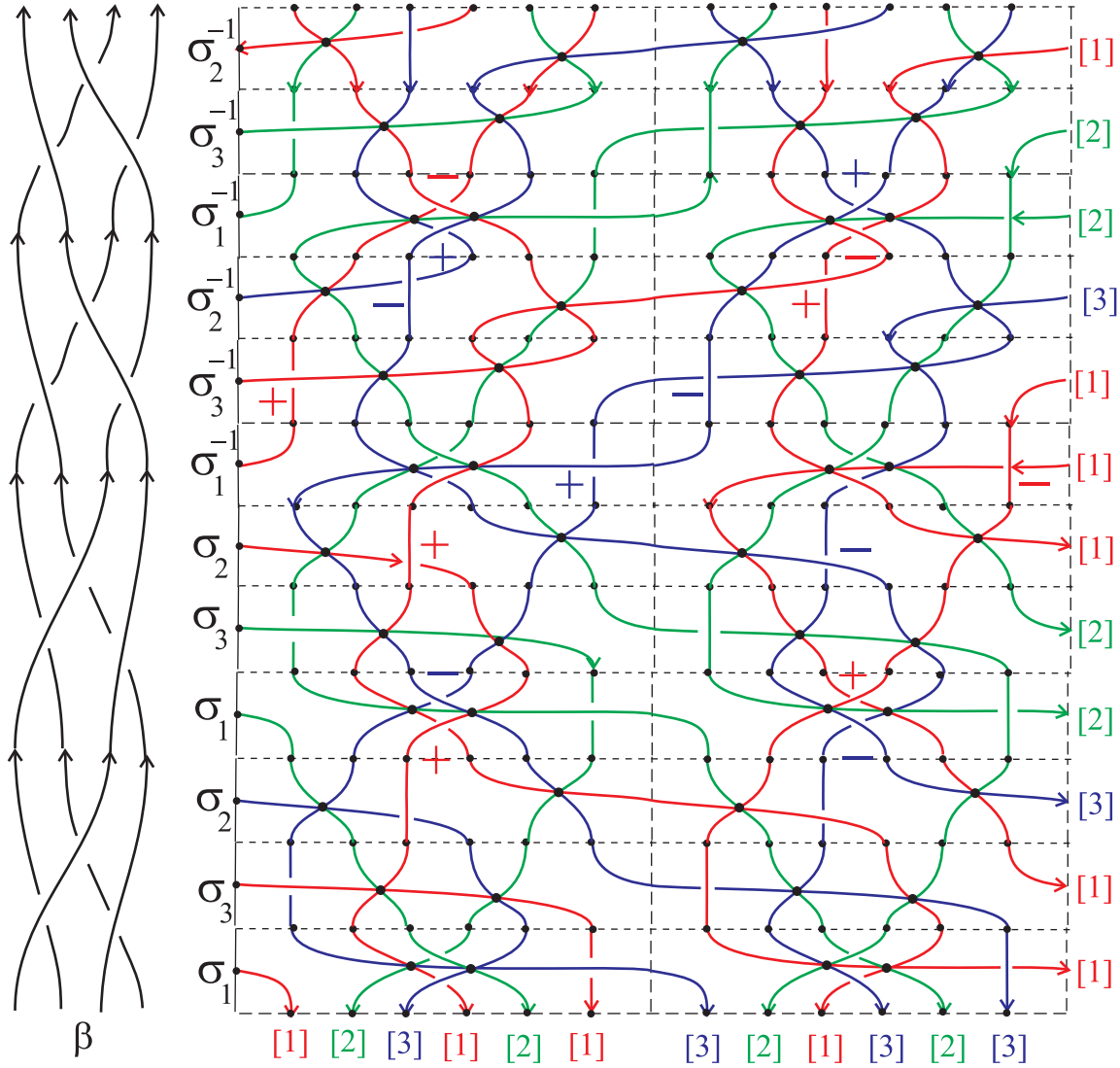


FIGURE 8. The part of the trace graph for the factor  $\beta = (\sigma_1\sigma_3\sigma_2)^2(\sigma_1^{-1}\sigma_3^{-1}\sigma_2^{-1})^2$ .

REFERENCES

- [1] J. S. Carter, M. Elhamdadi, M. Saito, S. Satoh, *A Lower Bound for the Number of Reidemeister Moves of Type III*, *Topology Appl.*, v. 153 (2006), 2788–2794.
- [2] E. Denne, Y. Diao, J. M. Sullivan, *Quadriseccants Give New Bounds for Ropelength*, *Geometry and Topology*, v. 10 (2006), 1–26.
- [3] T. Fiedler, V. Kurlin, *A One-parameter Approach to Knot Theory*, math.GT/0606381.
- [4] T. Fiedler, *Isotopy Invariants for Closed Braids and Almost Closed Braids via Loops in Stratified Spaces*, math.GT/0606443.

LABORATOIRE EMILE PICARD, UNIVERSITÉ PAUL SABATIER, 118 ROUTE NARBONNE, 31062 TOULOUSE, FRANCE

*E-mail address:* fiedler@picard.ups-tlse.fr

DEPARTMENT OF MATHEMATICAL SCIENCES, UNIVERSITY OF LIVERPOOL, LIVERPOOL L69 7ZL, UNITED KINGDOM

*E-mail address:* kurlin@liv.ac.uk, vak26@yandex.ru